



**HAL**  
open science

# Optimal Control Strategies for Energy Production Systems using Buildings Thermal Mass

Charbel Salameh, Patrick Schalbart, Bruno Peuportier

► **To cite this version:**

Charbel Salameh, Patrick Schalbart, Bruno Peuportier. Optimal Control Strategies for Energy Production Systems using Buildings Thermal Mass. Building Simulation 2021 Conference, Sep 2021, Bruges, Belgium. hal-03379993

**HAL Id: hal-03379993**

**<https://hal.science/hal-03379993v1>**

Submitted on 15 Oct 2021

**HAL** is a multi-disciplinary open access archive for the deposit and dissemination of scientific research documents, whether they are published or not. The documents may come from teaching and research institutions in France or abroad, or from public or private research centers.

L'archive ouverte pluridisciplinaire **HAL**, est destinée au dépôt et à la diffusion de documents scientifiques de niveau recherche, publiés ou non, émanant des établissements d'enseignement et de recherche français ou étrangers, des laboratoires publics ou privés.

# Optimal Control Strategies for Energy Production Systems using Buildings Thermal Mass

Charbel Salameh<sup>1,2</sup>, Patrick Schalbart<sup>1</sup>, Bruno Peuportier<sup>1</sup>

<sup>1</sup>MINES Paristech, PSL Research University, CES – Centre for energy efficiency of systems, Paris, France

<sup>2</sup>ACCENTA, Boulogne - Billancourt, France

## Abstract

The aim of this study is to develop real-time energy management strategies for HVAC systems taking into account the heat storage in building thermal mass. In fact, thermal energy production represents up to 50 % of building's total energy consumption and 75 % of Greenhouse Gases (GHG) emissions. Different systems and storage methods can be integrated to reduce the cost and the GHG emissions related to heating, cooling and Domestic Hot Water (DHW) production in buildings. In this context, multiple studies have developed optimal control systems (such as Model Predictive Control) for optimising thermal production and/or storage systems. The results presented in these studies showed a wide range of reduction rates due to different hypotheses, models, methods and systems taken into consideration. In real time optimisation, the building model is usually separated from the thermal system. In this study, a reduced model and a continuous optimisation method were used to minimise the cost of the building's heating. The applied strategy combined the building model and thermal mass with a Ground Source Heat Pump (GSHP) and a Borehole Thermal Energy Storage (BTES). This first approach showed promising results by reducing the cost between 10 % and 15 %. This method will be used to combine different systems and improve their performance in real-time.

## Key Innovations

- Real time simultaneous multi-system optimisation using Pontryagin Minimum Principle.
- BTES and GSHP operation optimisation taking into consideration building thermal mass energy storage under variable electricity pricing.

## Practical Implications

Real time optimal control is an interesting solution for cost and GHG emissions reduction. When it comes to such simulations, the results can vary on the models, hypotheses and algorithms used. Every project should be analysed separately, and the building properties taken into consideration in the application of the optimal control.

## Introduction

The building sector is the most energy-consuming sector in France, in particular, and in the world in general, it is also the second highest source of GHG emissions just behind transportation (Enerdata and ADEME 2018). This is mainly due to heating and air conditioning which contribute to the largest part of energy consumption especially in old buildings. There are two options for reducing energy consumption and GHG emissions while meeting the thermal comfort of building occupants: improving buildings' insulation or improving energy production systems.

In the design phase, the choice of construction materials, insulation and openings determines the quality of the envelope and thus, the coefficient of heat losses. New buildings are becoming more insulated, which leads to higher energy efficiency. In addition, the architecture takes more and more into account the orientation of the building's glazed surfaces, which –for instance- makes it possible to take advantage of external heat gains from the southern façade and to avoid heat losses from the northern side. As a result, energy production systems and their regulations have a greater impact on building energy performance and the residents' comfort.

On the thermal production side, having systems with a high coefficient of performance is one of many solutions to increasing energy efficiency. Coupling such systems with storage equipment (geothermal storage for instance) and managing this energy storage with a predictive controller makes it possible to optimise the production efficiency while minimising the overall thermal system cost. Indeed, such a controller can anticipate the best moment to use the energy storage, predicting the occupants' behaviour, the building needs and the thermal energy cost.

Energy consumption management or Demand Side Management (DSM) is another possible solution for reducing environmental impacts and energy bills. It consists of developing strategies to smooth out power consumption at peak hours (similar strategies can be applied to smooth out seasonal peaks). This is motivated by the fact that electricity is usually more expensive during these peaks and its production has a higher environmental impact (as the most polluting power station are switched on to supplement production).

The introduction of renewable energy in production systems is another solution for the reduction of electricity consumption and environmental impacts. The fact remains that these systems have their own inconvenience. In the case of solar energy, for example, there is a time difference between the moment it is available and the moment that it is needed. As for geothermal heat pumps, they extract (in heating mode) or inject (in cooling mode) energy from the BTES. In the absence of a balanced heating/cooling production or another system, the ground temperature is disturbed, leading to a reduction in the efficiency of the energy production.

In summary, the reduction of environmental impacts and energy consumption in the building sector can be achieved at different levels. The building envelope is the first phase, followed by the choice of the energy production system. The performance of the energy systems integrating renewable energy and storage strongly depends on the control that optimises the systems' operation.

Thermal energy storage can also be a solution, where energy is stored during off-peak hours or when it is available, in the case of renewable energy, then used when it is needed. The most common storage methods for buildings are batteries and thermal storage such as hot water tanks or ice tanks. Batteries are used with renewable electricity production like wind turbines and photovoltaic systems. They allow the integration of such systems in buildings. Bartolucci et al. (2019) studied a predictive control for a system combining photovoltaic panels and batteries. The study showed an 8.7 % cost reduction and 14.1 % decrease in grid unbalance. When it comes to thermal storage, Heier, et al. (2015) presented the different systems that can be combined with building energy production and we can identify two types: passive storage and active storage.

Passive storage is the use of the construction materials' thermal mass to store energy. In the case of passive storage, the building's inertia plays a major role in the storage capacity and peak erase. The stored energy is more important in a building with high inertia compared to a building with low inertia. This makes it possible to offset the consumption of heating during peak hours by storing energy during off-peak hours (Favre 2013). By using three different tariffs for off-peak, peak and rush hours, Robillart et al. (2019) managed to completely erase consumption during peak hours by using the thermal mass of a high-performance building while respecting the comfort constraints of the building's indoor temperature. Applying an MPC to optimise the temperature set point and integrating the total energy consumed and the maximal power demand as the target function, allows a reduction in peak demand between 15 % and 35 % (Braun 2003). By applying variable electricity rates with an MPC, Oldewurtel et al. (2010) reported a reduction of 7.9 % compared to constant rates. By making the same comparison (constant/variable electricity rates) on several types of buildings, Oldewurtel et al. (2011) deduced a reduction of 4 % to

19 %. The latter being for buildings with high thermal capacity.

Combining active storage with passive storage allows for further reduction of energy production costs. Considering the demand cost as the objective function in an MPC, in a building with an ice tank, a reduction in energy consumption during peak hours of 25 % is obtained with a 50 % reduction charge cost (Kircher and Zhang 2015). In order to control the building's energy demand and minimise power consumption during peak hours, Oldewurtel et al. (2011) developed an MPC to regulate the energy consumption of buildings with an electricity storage battery and compared the results for constant and variable electricity rates. A 15 % decrease in power demand during peak hours is noted when battery capacity exceeds 1kWh. Considering the cost of demand as an objective function, the peak electrical demand can be reduced by up to 40 % in buildings with high thermal capacity and ice storage (Hajiah and Krarti 2012a; Hajiah and Krarti 2012b).

The MPC's performance and the results obtained depend on the objective function. In addition, the following parameters are influential (Thieblemont et al. 2017):

- The thermal mass of the building.
- The capacity of the storage system.
- The climate.
- The electricity tariff.
- Comfort constraints.
- The optimisation horizon.
- The assumptions of the simulation scenarios.

Besides, an MPC allows better management of renewable energies by anticipating the needs and production of renewable energy systems. Studies have shown a 50 % increase in the use of renewable energies by applying an MPC to commercial buildings (Zong et al. 2012; Mayer et al. 2016).

The difficulties of installing an MPC can be divided into two categories: modelling and optimisation of the system (building and / or storage system) and the uncertainty of assumptions and predictions.

In this paper, an indirect method is applied to solve the optimisation problem as a foundation for developing a predictive control minimising the cost of the heating and cooling production while combining the building model with the BTES model. This approach will not only allow the energy production to maintain the comfort in the building but will also take into consideration the BTES temperature and its impact on the GSHP Coefficient Of Performance (COP).

## Case Study

A house from the INCAS platform, shown in Figure 1, located in Bourget-du-Lac (France) has been chosen as the case study. It serves as the basis for comparing the application of an optimal control strategy for an electric heating system with a constant efficiency equal to 1, which will be the subject of the first simulation. The second simulation will be for the same building with a GSHP energy production system.

The house has two floors and has a surface of 89 m<sup>2</sup>. It has a high-quality envelope, well insulated on the exterior surface and high performance glazing. External walls are built of 15 cm concrete with 20 cm insulation of extruded polystyrene. The ground slab is made of 20 cm concrete and 20 cm external polystyrene insulation.



The insulation in the attic is of 40cm glass wool. The northern windows are triple glazing while the other façades have double glazing windows. The building model consists of a single zone.

Figure 1: INCAS house

The constraints of this system relate to the comfort temperature and the power of the installed heating system:

- State constraints:

$$T_{min} \leq T_{zone}(t) \leq T_{max} \quad (1)$$

with:  $T_{min}=19^{\circ}\text{C}$  et  $T_{max}=23^{\circ}\text{C}$

- Control constraints:

$$\dot{Q}_{hmin} \leq u(t) \leq \dot{Q}_{hmax} \quad (2)$$

with:  $\dot{Q}_{hmin} = 0$  kW et  $\dot{Q}_{hmax} = 5$  kW for the heating power.

Figure 2 shows the outside temperature and the solar radiation data of the coldest week in January during which the simulation was applied. Figure 3 shows the internal heat gains for a typical simulation day.

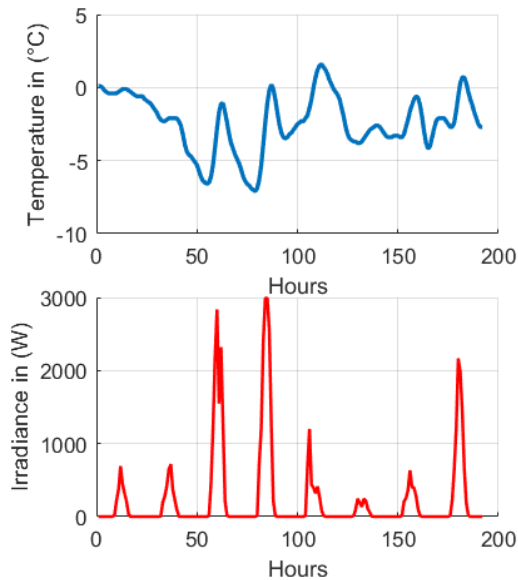


Figure 2: Weather data for the coldest week

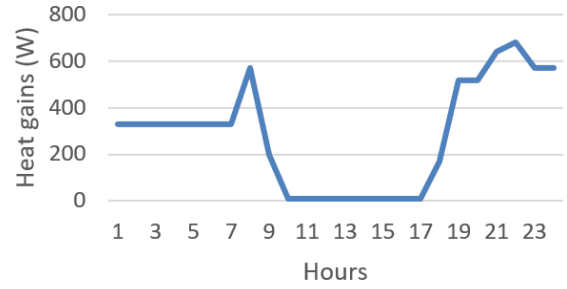


Figure 3: Internal heat gains

In order to allow the heat storage in the building thermal mass and shift electricity consumption from peak and high peak hours to off-peak periods, three different electricity rates have been used (Table 1).

Table 1: Electricity rates

	Off peak	peak	high peak
Period	0h-9h	9h-17h 22h-0h	17h-22h
Cost of kWh in €	0.0864	0.1275	0.255

## Models

In the first simulation, a perfect electric heater is considered.

For the second simulation, and as a first approach, we optimise energy storage and consumption using both the building and the BTES dynamics (considering the impact of heat production on GSHP efficiency). The heating is considered to be injected directly in the zone. The system consists of a geothermal heat pump connected to the BTES, which makes it possible to extract and store energy in the ground. The goal is to meet the energy building needs at optimal cost. Dynamic thermal models representing the building and the heat pump are required to compute optimal control.

### Thermal model of the building

The thermal model of the building is obtained from the dynamic building energy simulation software Pleiades<sup>1</sup>. This allows calculating the temperature of thermal zones by establishing the thermal balance for each mesh making up the zone. The integrated building model, COMFIE, is based on the work presented by Peuportier and Sommereux (1990). For each zone, the walls are divided into meshes (finite volume method) on which a thermal balance is applied assuming that the temperature of the mesh is uniform. To ensure this assumption, the mesh is finer as it gets closer to the thermal zone. The air, furniture and any light partitions contained in the area are grouped together in a single mesh. The heat balance on each mesh then takes the following form (Neveu 1984):

<sup>1</sup> <https://www.izuba.fr/>

$$C_m \frac{dT_m}{dt} = \dot{Q}_G - \dot{Q}_P \quad (3)$$

with

- $C_m$  the thermal capacity of the mesh.
- $T_m$  the temperature of the mesh.
- $\dot{Q}_G$  the solar and internal gains, including the heating or cooling capacities of equipment.
- $\dot{Q}_P$  the thermal losses due to ventilation and heat transfer by conduction, convection, radiation.

Some non-stationary (opening of shutters) or non-linear (air movement) phenomena are taken into account in the vector denoted  $U$ , which makes it possible to write the equations (3) in the form of a system linear equations with constant coefficients (4).

By repeating this thermal balance equation for each mesh in the zone and adding an output, the equations can thus be represented in the form of a continuous and invariant linear system (Bacot 1984; Lefebvre 1987):

$$\begin{cases} C\dot{T}(t) = AT(t) + EU(t) \\ Y(t) = JT(t) + GU(t) \end{cases} \quad (4)$$

with

- $T$  discretised vector of mesh temperatures;
- $C$  diagonal matrix presenting thermal capacities
- $U$  solicitation vector (including climate parameters, heating, etc.)
- $A$  state matrix (exchange inter-mesh)
- $E$  input matrix (exchange between the mesh and solicitations)
- $J$  observation matrix
- $G$  direct action matrix
- $Y$  output vector (indoor temperature of the zone considering air and walls surface).

The simulation of this model requires the knowledge of the solicitations, (internal heat gains of the occupants and the equipment) and weather data (outdoor temperature and solar radiation). All of this data is contained in the solicitation vector. The building model for the case study consists of 29 states.

Model reduction is achieved through balanced realisation, hence reducing computation time. This method seeks to optimise the degrees of observability and controllability of the system. Following the balanced realisation, a truncation is applied by eliminating states associated with the small Hankel singular values (Robillart et al. 2019).

### Thermal model of the boreholes

A simplified reduced model derived from a detailed model was used in the simulations. Based on the method developed by Zeng et al. (2003), the heat transfer inside the borehole can be calculated taking into consideration the convective transfer of the fluid inside the borehole. As for the modelling of the outside surface temperature of the borehole for the detailed model, three methods are used in order to determine the surface temperature based on the simulation period. For few days periods the infinite line source method, for couple of years periods the infinite cylinder source method and for periods

longer than those, the finite line source method is applied.

Based on these models, the equations of the simplified model representing the temperature variation of the ground and at the surface of the borehole can be expressed as a linear dynamic system with the form:

$$dT = aT + b\dot{q} \quad (5)$$

with  $T$  representing the temperatures vector in the ground noted  $T_2$  and on the surface of the borehole noted  $T_1$ ,  $a$  and  $b$  the coefficients representing the properties of the transfer between the borehole and the ground, and the borehole and the fluid,  $q$  the heat extracted from the borehole by the GSHP. The parameters  $a$  and  $b$  were calculated in a way to minimise the error between the complete model and the simplified model. The BTES and GSHP models and parameters are based on Accenta<sup>2</sup>'s system.

### Thermal model of the GSHP

By definition, the coefficient of performance of heat pumps is the ratio between the thermal power supplied by the heat pump ( $\dot{Q}_h$ ) and the electrical power ( $\dot{W}_e$ ) consumed:

$$COP = \frac{\dot{Q}_h}{\dot{W}_e} \quad (6)$$

Figure 4 illustrates the operation, in heating mode, of the geothermal heat pump.

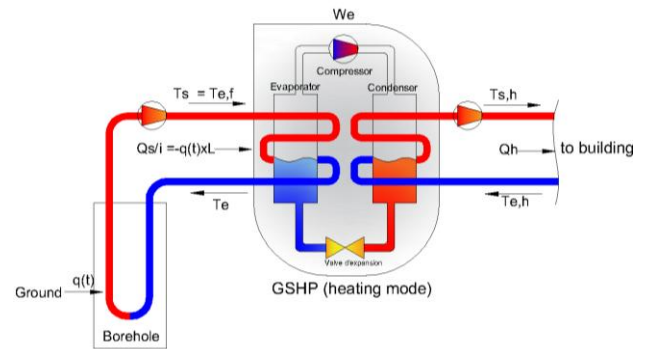


Figure 4: Ground Source Heat Pump model

By neglecting geothermal heat pump thermal losses and auxiliary consumption, the power injected or withdrawn from the borehole ( $\dot{Q}_{s/i}$ ) is calculated by the equation:

$$\dot{Q}_{s/i} = \left[ \dot{Q}_h - \frac{\dot{Q}_h}{COP} \right] \quad (7)$$

The coefficient of performance of the heat pump is determined as follows:

<sup>2</sup> <https://www.accenta.ai>

$$COP_{PAC} = \eta_{PAC} \times COP_{carnot} \quad (8)$$

As for the heating mode,  $COP_{carnot}$  is:

$$COP_{carnot} = \frac{T_{e,h}}{T_{e,h} - T_{e,f}} \quad (9)$$

with

- $COP_{carnot}$ , COP at maximum efficiency (ideal Carnot cycle)
- $\eta_{PAC}$ , actual efficiency of heat pump cycle compared to the Carnot cycle taking into account heat losses and referring to the technical data sheets (considered constant for this simulation)
- $T_{e,h}$ , temperature of the fluid at the inlet of the hot source
- $T_{e,f}$ , temperature of the fluid at the inlet of the cold reservoir.

The expression of the temperature of the fluid at the outlet of the borehole ( $T_s$ ) in terms of the heat exchange  $\dot{q}(t)$  from (5) is calculated based on the following equation:

$$T_s = T_1(t) + R\dot{q}(t) + \frac{\Delta T}{2} \quad (10)$$

with

- $T_e$ , the temperature of the fluid at the inlet of the borehole.
- $T_s$ , the temperature of the fluid at the outlet of the borehole.
- $R$ , the thermal resistance between the fluid circulating in the tube and the borehole surface.
- $\Delta T$ , the difference between the temperature of the fluid at the inlet  $T_e$  and the outlet  $T_s$  of the borehole

$\Delta T$  is considered constant at 3°C but the fluid mass flow rate is controlled and variable

The total power exchanged between the fluid and the BTES is of the form:

$$\dot{q}(t) * L = \dot{m}c(T_e - T_s) \quad (11)$$

with:

- $L$ , the total borehole length.
- $\dot{m}$ , the mass flow rate of the fluid.
- $c$ , the specific heat of the fluid.

Based on the equations (8), (9), (10) and (11) we can establish the equation of the COP as follows:

$$\frac{1}{COP^2} + (-\alpha + \beta * T_1 + \delta * \dot{Q}_h) * \frac{1}{COP} - \delta * \dot{Q}_h = 0 \quad (12)$$

$$\text{with: } \alpha = \frac{1}{\eta} \left(1 - \frac{\Delta T}{2T_{e,h}}\right); \beta = \frac{1}{\eta T_{e,h}}; \delta = \frac{R}{\eta 4T_{e,h}L}.$$

## Methods

### Optimal control

The aim of optimal control, related to the energy management of buildings, is to optimise a criterion (objective function) such as energy production cost to meet building thermal comfort needs (state constraints).

Optimal control consists in solving an optimisation problem by minimising the objective function under state or control constraint. For buildings, the optimal

control can be used to determine the best control with the energy production cost and storage as the objective function (heating or air conditioning) as well as GHG emissions. In this study, we consider minimising the cost of the energy production. Noting that the same method can be applied for the GHG emissions by substituting the cost function. The coupling of the production and storage system with the thermal mass of the building is carried out taking into account the solicitations and constraints of temperature (state) and power (control).

The general problem of optimal control without constraint can be written as:

$$\min_{u \in U} \left[ J(u, x) = \int_0^{t_f} L(x(t), u(t)) dt \right] \quad (13)$$

with  $L$  a regular real-value function,  $x$  the state and  $u$  the control. The general form of the differential equation that represents the dynamics of the system and the variation of the state in terms of the control is:

$$\dot{x}(t) = f(x^u(t), u(t)) ; x(0) = x_0 \quad (14)$$

There are two main approaches to solve the problem of optimal control: the Pontryagin Minimum Principle (PMP) and dynamic programming (Bellman optimisation principle).

In this study, based on the algorithm developed in Robillart et al. (2019) for an electrical heater, the Pontryagin Minimum Principle was applied. In fact, the PMP states the necessary conditions for optimality by solving the Hamiltonian system. The problem is then a two-point boundary value problem. The general form of the Hamiltonian is defined as:

$$\begin{aligned} H(x(t), u(t), p(t)) \\ &= L(x(t), u(t)) \\ &+ p(t)Tf(x(t), u(t)) \end{aligned} \quad (15)$$

If  $(u, x) \in U \times \mathbb{R}^n$  is a solution of the optimisation problem, there exists an adjoint state defined by  $p(t): [0; t_f] \rightarrow \mathbb{R}^n$  for almost all  $t \in [0; t_f]$  such as:

$$\dot{x}(t) = f(x(t), u(t)), x(0) = x_0 \quad (16)$$

$$\dot{x}^*(t) = \frac{\partial}{\partial p} H(x^*(t), u^*(t), p(t)) \quad (17)$$

$$\begin{aligned} \dot{p}^T(t) &= \frac{\partial}{\partial x} H(x^*(t), u^*(t), p(t)) \\ p^T(t_f) &= 0 \end{aligned} \quad (18)$$

$$\begin{aligned} H(x^*(t), u^*(t), p(t)) \\ &= \min_u H(x^*(t), u(t), p(t)) \end{aligned} \quad (19)$$

$x^*$  being the solution of the optimisation problem.

In order to respect the limits of the temperature and control in the simulation, an interior penalty method was applied. The constraints on the state and control are expressed in the form of interior penalisation and the Hamiltonian of the penalised problem becomes (Malisani et al. 2016):

$$\begin{aligned}
H(x(t), u(t), p(t)) &= L(x(t), u(t)) \\
&+ p^T f(x(t), u(t)) \\
&+ \varepsilon_x [\gamma_g (Cx - T_{min}) \\
&+ \gamma_g (T_{max} - Cx)] \\
&+ \varepsilon_u [\gamma_u (u - U_{min}) \\
&+ \gamma_u (U_{max} - u)]
\end{aligned} \quad (20)$$

$\gamma_g$  and  $\gamma_u$  being the penalty functions of the state and the control respectively.

Applying this method to the case study, the objective function that minimises the energy cost is defined as:

$$\min_{u \in U} \left[ J(u, x) = \int_0^{t_f} Er(t) * W_e(t) dt \right] \quad (21)$$

with:

- $Er$ , electricity rates vector.
- $W_e$ , the GSHP electrical power consumption.

Equations (4) and (5) can be written under the form:

$$\dot{x}(t) = A_r x + B_r U + g(COP) * \dot{Q}_h \quad (22)$$

where  $x$  is the state vector including the reduced state of the building and the BTES temperatures,  $A_r$  the state matrix,  $B_r$  the input matrix  $g(COP)$  function of the COP.

The Hamiltonian associated to this problem becomes:

$$\begin{aligned}
H &= Er(t) * We(t) \\
&+ p^T (A_r x + B_r U \\
&+ g(x, \dot{Q}_h) * \dot{Q}_h) \\
&+ \varepsilon_x [\gamma_g (Cx - T_{min}) \\
&+ \gamma_g (T_{max} - Cx)] \\
&+ \varepsilon_u [\gamma_u (u - U_{min}) \\
&+ \gamma_u (U_{max} - u)]
\end{aligned} \quad (23)$$

The algorithm was coded in MATLAB using the boundary value solver function `bvp5c` that applies a collocation method in order to solve the differential equations of the state and the adjoint state.

## Results

### Electric heating

The optimisation was tested on a project having an electric heater to validate the model and to serve as a basis of comparison to the model coupled with the variable COP of the GSHP. The latter presents the control of the building to be optimised. In the case of the electric heater, optimal control allows full shift of peak and peak hours (Figure 5, Figure 6). The optimisation strategy makes it possible to store thermal energy in the mass of the building during the cheapest off-peak hours and restore it in the zone during the most expensive hours. During off-peak hours, the indoor temperature increases to a maximum of 22.5°C. The temperature will decrease in the hours when the heating is turned off to apply the shift. The temperature's upper and lower limits are respected over the optimisation horizon ensuring the thermal comfort.

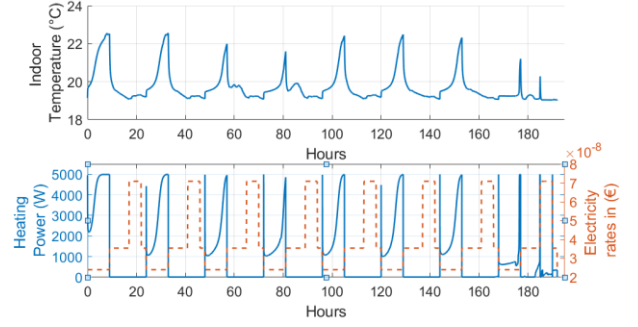


Figure 5: Optimisation of electric heater for one week

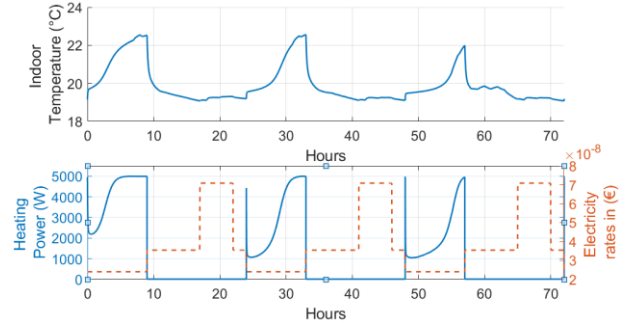


Figure 6: Zoom in on three days

A traditional heating control that is programmed to keep a constant setpoint is shown in Figure 7. The heating system provides energy to respect a minimum indoor temperature at 19.1°C. Comparing the two strategies, optimal control provides more energy and requires higher production power during off-peak hours. Obviously storing the additional energy in the building mass requires the system to exceed the heating needs. However, based on the electricity rates and comparing the energy consumption cost for this week, a 26 % decrease in the heating cost was observed.

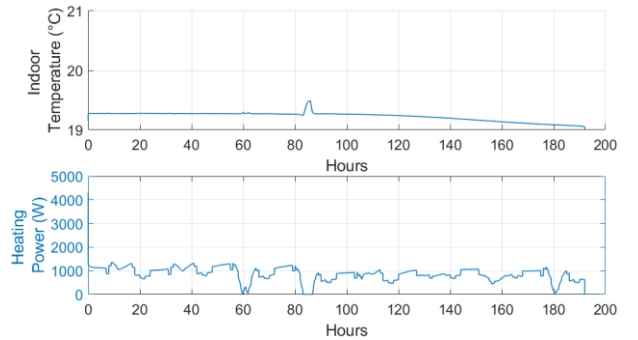


Figure 7: Traditional heating control

Table 2 presents a summary of the heating energy produced and the cost at the seventh day of optimisation (last day was not included to neglect the boundary effect of the optimisation).

Table 2: Energy and cost for electric heating

	Traditional IDEAL Control	Optimised Control
Heating Energy kWh	148	167

Cost €	19.5	14.4
--------	------	------

### GSHP

Then the system coupled with the variable GSHP COP model is simulated. The GSHP COP depends on the ground temperature. Variation in the temperature of the geothermal storage depends on the energy withdrawn / injected into the ground and therefore, on the heating power. In this first approach, and in order to speed up the calculation, the variation in soil temperature is assumed negligible during one-week optimisation horizon. In order to optimise the following period, the soil temperature should be simulated and updated based on the previous optimisation. The variation of the COP, for each horizon, depends directly on the heating power in the building. The temperature and heating power profiles are shown in Figure 8 and Figure 9. The COP profile is shown in Figure 10. The COP profile applied is theoretical and does not represent real values of a GSHP operation. In real time applications, this model is replaced by real data.

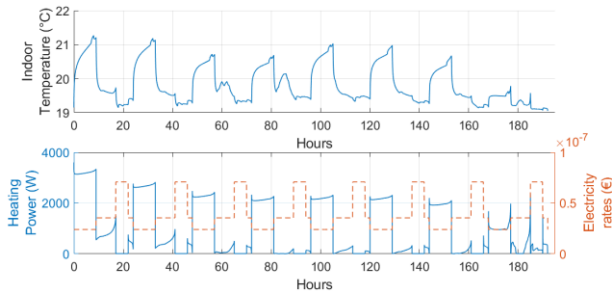


Figure 8: Optimisation combining the GSHP and building model

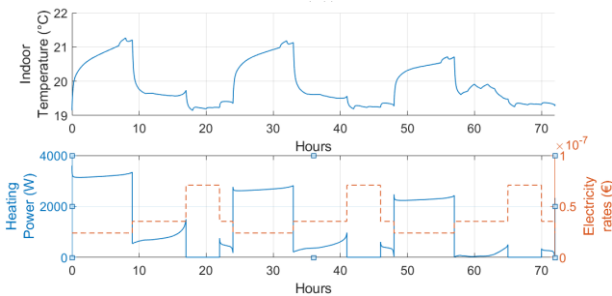


Figure 9: Zoom in on three days

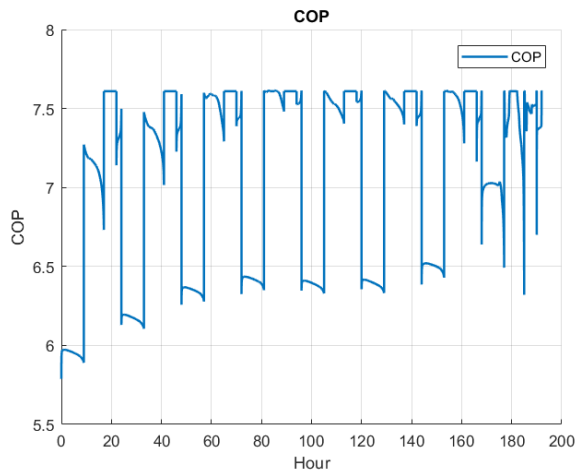


Figure 10: COP

In this case, both geothermal storage operation and the building heating needs are coupled and optimised taking into account the building's thermal mass. Note that the consumption shift to off-peak hours is not total as in the first example. The withdrawal of energy from the ground storage causes a decrease in the COP, which justifies the lower power production during off-peak hours in this case. The energy stored in the building is therefore lower than with the electric heater example. In order to respect the constraints of the minimum comfort temperature, the optimal solution consists of heating the building during peak hours as well. Note that the maximum reached temperature, 21.3°C, is also lower than that in the first simulation. As the COP varies inversely with the amount of power consumed, the minimisation of the operating cost becomes a compromise between total energy consumption shift (maximum power demand during off-peak hours) and partial shift, which makes it possible to maintain optimal system efficiency.

Table 3 presents a summary of the heating energy produced and the cost at the seventh day for the GSHP system simulation and we noticed a 20 % decrease for the heating cost.

Table 3: Energy and cost for GSHP

	Traditional GSHP	Optimised GSHP
Heating Energy kWh	148	167
Cost €	2.9	2.3

### Conclusion

Optimal control has been applied to the heating of a high performance building in order to minimise the cost of the energy production and maximise the efficiency of the heat storage and the production system, in this case a GSHP and a BTES. As a first approach, an electric heater was considered to highlight the benefits of applying such methods to the building heating control with variable electricity rates. The results showed a total energy consumption shift from peak and rush hours to off-peak hours. The energy produced and stored in the building mass during off-peak hours allowed the temperature to remain over the lower limit during the other periods without requiring any active heating. When it comes to geothermal boreholes coupled with a heat pump production system, the GSHP COP depends on the ground temperature. In heating mode, the GSHP extracts heat from the ground causing the soil temperature to decrease. This explains the results obtained when applying optimal control where the solution did not consist in applying a total energy consumption shift to off-peak hours. This study presents an optimal control strategy combining different systems while optimising the building needs. Further work will consist in simulating an MPC over a year then over 20 years to determine the effects of heating and cooling on the ground dynamics, in particular when the cooling and



heating needs are not balanced. In addition, other energy production systems will be added, i.e. Air Source Heat Pump (ASHP) or solar heating. This will allow efficient energy production, maintaining the balance in the ground temperature by storing the additional produced energy in the ground. This method can also be applied to minimise the energy production cost and/or the GHG emissions.

## Acknowledgement

This study was possible due to the support and financing of Accenta in collaboration with CES Mines-Paristech.

## References

- Bacot, Patrick. 1984. "Analyse Modale Des Systèmes Thermiques." École Nationale Supérieure des Mines de Paris.
- Bartolucci, Lorenzo, Stefano Cordiner, Vincenzo Mulone, and Marina Santarelli. 2019. "Short-Term Forecasting Method to Improve the Performance of a Model Predictive Control Strategy for a Residential Hybrid Renewable Energy System." *Energy*, January. doi:10.1016/j.energy.2019.01.104.
- Braun, James E. 2003. "Load Control Using Building Thermal Mass." *Journal of Solar Energy Engineering* 125 (3): 292. doi:10.1115/1.1592184.
- Enerdata, and ADEME. 2018. "Ademe - Climat Air et Energie chiffres clés." [https://www.ademe.fr/sites/default/files/assets/documents/2018-climat-air-energie\\_chiffres-cles-010354.pdf](https://www.ademe.fr/sites/default/files/assets/documents/2018-climat-air-energie_chiffres-cles-010354.pdf).
- Favre, Bérénger. 2013. "Étude de stratégies de gestion énergétique des bâtiments par l'application de la programmation dynamique," 285.
- Hajiah, Ali, and Moncef Krarti. 2012a. "Optimal Control of Building Storage Systems Using Both Ice Storage and Thermal Mass – Part I: Simulation Environment." *Energy Conversion and Management* 64 (December): 499–508. doi:10.1016/j.enconman.2012.02.016.
- Hajiah, Ali, and Moncef Krarti. 2012b. "Optimal Controls of Building Storage Systems Using Both Ice Storage and Thermal Mass – Part II: Parametric Analysis." *Energy Conversion and Management* 64 (December): 509–515. doi:10.1016/j.enconman.2012.02.020.
- Heier, Johan, Chris Bales, and Viktoria Martin. 2015. "Combining Thermal Energy Storage with Buildings – a Review." *Renewable and Sustainable Energy Reviews* 42 (February): 1305–1325. doi:10.1016/j.rser.2014.11.031.
- Kircher, Kevin J., and K. Max Zhang. 2015. "Model Predictive Control of Thermal Storage for Demand Response." In *2015 American Control Conference (ACC)*, 956–961. Chicago, IL, USA: IEEE. doi:10.1109/ACC.2015.7170857.
- Lefebvre, Gilles. 1987. "Analyse et Réduction Modales d'un Modèle de Comportement Thermique Du Bâtiment." Université Pierre et Marie Curie, Paris VI.
- Malisani, P., F. Chaplais, and N. Petit. 2016. "An Interior Penalty Method for Optimal Control Problems with State and Input Constraints of Nonlinear Systems." *Optimal Control Applications and Methods* 37 (1): 3–33. doi:10.1002/oca.2134.
- Mayer, Barbara, Michaela Killian, and Martin Kozek. 2016. "A Branch and Bound Approach for Building Cooling Supply Control with Hybrid Model Predictive Control." *Energy and Buildings* 128 (September): 553–566. doi:10.1016/j.enbuild.2016.07.027.
- Neveu, Alain. 1984. "Étude d'un Code de Calcul d'évolution Thermique d'une Enveloppe de Bâtiment." Université Pierre et Marie Curie, Paris VI.
- Oldewurtel, Frauke, Andreas Ulbig, Manfred Morari, and Goran Andersson. 2011. "Building Control and Storage Management with Dynamic Tariffs for Shaping Demand Response." In *2011 2nd IEEE PES International Conference and Exhibition on Innovative Smart Grid Technologies*, 1–8. Manchester, United Kingdom: IEEE. doi:10.1109/ISGTEurope.2011.6162694.
- Oldewurtel, Frauke, Andreas Ulbig, Alessandra Parisio, Goran Andersson, and Manfred Morari. 2010. "Reducing Peak Electricity Demand in Building Climate Control Using Real-Time Pricing and Model Predictive Control." In *49th IEEE Conference on Decision and Control (CDC)*, 1927–1932. Atlanta, GA, USA: IEEE. doi:10.1109/CDC.2010.5717458.
- Peuportier, Bruno, and Isabelle Blanc Sommeux. 1990. "SIMULATION TOOL WITH ITS EXPERT INTERFACE FOR THE THERMAL DESIGN OF MULTIZONE BUILDINGS." *International Journal of Solar Energy* 8 (2): 109–120. doi:10.1080/01425919008909714.
- Robillart, M., P. Schalbart, F. Chaplais, and B. Peuportier. 2019. "Model Reduction and Model Predictive Control of Energy-Efficient Buildings for Electrical Heating Load Shifting." *Journal of Process Control* 74 (February): 23–34. doi:10.1016/j.jprocont.2018.03.007.
- Thieblemont, Hélène, Fariborz Haghighat, Ryoza Ooka, and Alain Moreau. 2017. "Predictive Control Strategies Based on Weather Forecast in Buildings with Energy Storage System: A Review of the State-of-the Art." *Energy and Buildings* 153 (October): 485–500. doi:10.1016/j.enbuild.2017.08.010.
- Zeng, Heyi, Nairen Diao, and Zhaohong Fang. 2003. "Heat Transfer Analysis of Boreholes in Vertical Ground Heat Exchangers." *International Journal of Heat and Mass Transfer* 46 (23): 4467–4481. doi:10.1016/S0017-9310(03)00270-9.

Zong, Yi, Daniel Kullmann, Anders Thavlov, Oliver Gehrke, and Henrik W. Bindner. 2012. "Application of Model Predictive Control for Active Load Management in a Distributed

Power System With High Wind Penetration." *IEEE Transactions on Smart Grid* 3 (2): 1055–1062. doi:10.1109/TSG.2011.2177282.